

富山大学水素同位体科学研究センター研究報告 21: 61-72, 2001.

## 論文

### SS-316 ステンレス鋼からのトリチウムの除染(I)

A. Perevezentsev<sup>1)</sup>, 渡辺国昭<sup>2)</sup>, 松山政夫<sup>2)</sup>, 鳥養祐二<sup>2)</sup>

1) UKAEA, Culham Science Centre, Abingdon, OX14 3DB, UK

2) 富山大学 水素同位体科学研究センター  
〒930-8555 富山市五福 3090

### Removal of tritium from stainless steel type 316(I)

A. Perevezentsev<sup>1)</sup>, K. Watanabe<sup>2)</sup>, M. Matsuyama<sup>2)</sup>, Y. Torikai<sup>2)</sup>

1) UKAEA, Culham Science Centre, Abingdon, OX14 3DB, UK

2) Hydrogen Isotope Research Center, Toyama University, Gofuku, Toyama 930-8555, Japan  
(Received November 5, 2002; Accepted December 20, 2002)

### Abstract

Tritium distribution in stainless steel type 316 exposed to tritium-containing hydrogen at various temperatures was studied. Sub-surface layer of approx. 20 $\mu$ m thickness enriched with tritium was observed for all samples. This layer contributes 20% to 40% to overall tritium inventory. Thermal desorption study reveals that majority of tritium released from the contaminated steel is in a form of water.

Several method of decontamination, such as purge with various gases at elevated temperatures and heating with methane-air flame, were tested. Heating with flame allows removal of largest fraction of tritium inventory and in shortest period of time among the tested decontamination methods.

## 1. Introduction

Maintenance and decommissioning of deuterium-tritium burning fusion reactors would require detritiation of stainless steel, which is a most common material of the tritium handling facilities [1]. The JET machine presents an example of such need [2]. The feature of stainless steel contamination by tritium is a large mobility of the contaminant. For example, tritium was found in the bulk of stainless steel exposed to gaseous tritium-containing hydrogen at room temperature [3]. Tritium demonstrated [4,5] so-called “re-growth” effect of re-appearing at the decontaminated surface. This indicates that being a mobile contaminant tritium can migrate in stainless steel quite easily even at moderated temperatures.

Another feature of tritium contamination of stainless steel is a form in which it is released. Thermal desorption studies of stainless steel exposed to gaseous tritium-containing hydrogen show that majority of tritium is released in a form of water vapor [1, 6-10].

Knowledge of tritium behavior in stainless steel is important for safety of operation and decommissioning of tritium handling facilities and future fusion reactors. Availability of an effective detritiation technique is a vital for reduction of the decommissioning cost caused by need for the waste disposal. The most commonly considered methods for detritiation are washing, thermal desorption, isotopic exchange, chemical and electrochemical etching, plasma discharge and destructive techniques, such as melting [1]. If decontamination of intermediate level waste (ILW) could reduce their activity below low level waste (LLW) threshold, this could lead to a substantial reduction in cost of the waste disposal. However, where detritiation of ILW using a simple and cheap technique of tritium recovery leads to generation of a sophisticated “mixed” chemical and radiological “secondary” waste, that needs to be processed as well, the overall cost of decontamination process could make it not cost-effective.

This paper reports first results of study of stainless steel type 316 detritiation by non-destructive methods.

## 2. Experimental

### 2.1 Samples preparation

Planchettes of SS316 of 15x15mm square shape and 0.6mm thickness (supplied by Metalfast, UK) were used as delivered. The only treatment was cleaning by ultrasonic bathing in acetone. The samples were placed in a quartz reactor attached to a high vacuum system. The reactor was pumped for several days at room temperature and residual gas pressure of  $\approx 10^{-6}$ Pa. The samples were heated then at 670K for 3 hours under vacuum of  $\approx 10^{-5}$ Pa and pumped again for several days at room temperature. Residual gas analysis shows that main impurity was water, which content was considerably reduced after the reactor heating. Samples were loaded with tritium by exposure to 1kPa of hydrogen containing 32% tritium. Prior to withdraw of the samples to ambient atmosphere the reactor was pumped for several days at room temperature. List of samples is given in Table 1.

**Table 1** List of samples loaded with tritium.

Sample series	Temperature and duration of exposure to tritium	Heat treatment after exposure <sup>b)</sup>
I	≈295K, 20 hours	None
II	470K, 3 hours	None
III	590K, 3 hours	None
IV	590K, 3 hours	720K, 5 hours
V <sup>a)</sup>	590K, 3 hours	770K, 10 hours

a) Samples were of 10x10mm size with 4.8mm thickness.

b) Samples loaded with tritium were baked-out in evacuated and valved off reactor.

## 2.2 Analysis of tritium distribution and release

Tritium distribution in the samples was evaluated by their acid etching followed by liquid scintillation counting of tritium in the acid cocktail. Etching cocktail, which is effective for whole surface corrosion and oxidation of desorbed hydrogen [8,11], contained 6.6w% HNO<sub>3</sub> and 10.9w% HCl in water. It was assumed that all tritium, independently of form in which it is presented in the sample, was oxidised during the etching and converted to water.

Thermal desorption study was used for assessment of chemical forms in which tritium can be released from the samples. Schematic of the test facility is given in Fig.1. Sample of stainless steel was loaded into quartz reactor, which was purged with argon of high purity grade, containing <0.1ppm of oxygen and <0.2ppm of methane. Reactor was heated at rate of 2K/min. Gas flow rate was 0.1NL/min, which is equivalent to gas velocity of ≈0.01m/s. Gas passes the reactor, a water bubbler, a molecular sieve trap, a reactor with copper oxide maintained at temperature of 970K for conversion of molecular hydrogen and hydrocarbons to water, and a second water bubbler. Efficiency of HTO trapping in a water bubbler was measured 99.5%. The facility shown in Fig.1 was also used for measurement of rate of tritium out-gassing from the samples under air at ambient temperature. Relative humidity of the air was usually of ≈25% at a temperature of 295K. Separate reactors and bubblers were used for samples of large and small rate of tritium out-gassing.

## 2.3 Decontamination tests

The following methods of detritiation were tested:

- a) Purging with ambient air at an elevated temperature.
- b) Purging at an elevated temperature with pure argon or argon containing either 10.0% of NH<sub>3</sub> or 3.1% of H<sub>2</sub>.
- c) Heating by methane – air flame with simultaneous purging with ambient air.

The facility shown in Fig. 1 was used for decontamination tests with the gas-purge. No copper oxide reactor was employed in the tests with argon containing NH<sub>3</sub> or H<sub>2</sub>. To reduce influence of a reactor “memory” on results of tritium release measurement, the test reactor was cleaned prior to each decontamination test by purging with the relevant tritium-free purge-gas at temperature

200K higher than that of the test. Amount of tritium released from the reactor during cleaning runs never exceeded 1% of amount of tritium released from the sample in the following decontamination test. For decontamination by flame, the sample was placed in an open-end quartz reactor purged by pumping via three consecutive bubblers connected to another end of the reactor. Air flow rate through the reactor was  $\approx 4\text{NL}/\text{min}$ . The reactor was installed inside secondary containment. No tritium was observed outside of the secondary containment.

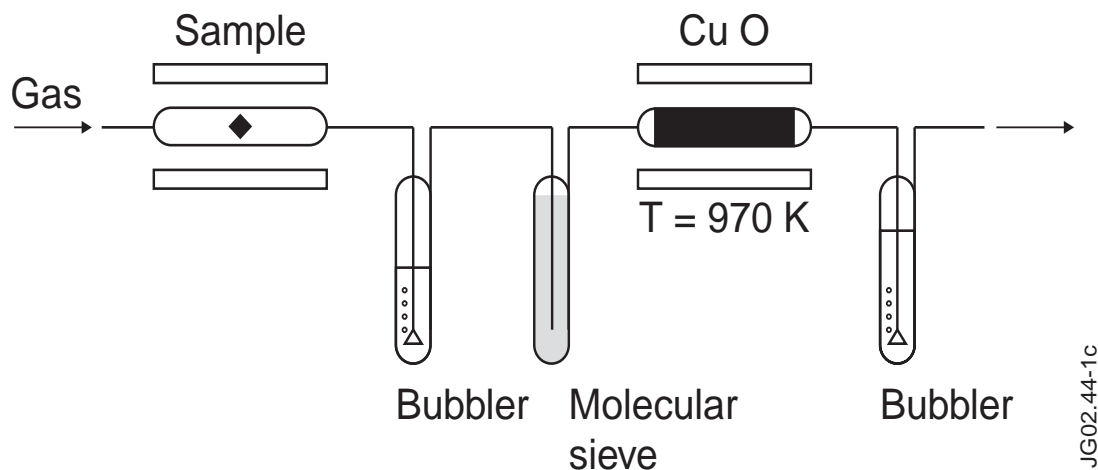


**Fig. 1** Schematic of experimental facility.

### 3. Results and discussion

#### 3.1 Tritium distribution in original samples

Table 2 presents the tritium inventory of the samples, tritium concentration in the surface layer and in the bulk. The overall tritium inventory was evaluated as a sum of tritium recovered from the samples during their decontamination and tritium left in the decontaminated samples and then measured by their chemical etching. The tritium depth profiles are presented in Fig. 2.

**Table 2** Distribution of tritium inventory in samples.

Sample series	Tritium Inventory MBq	Tritium concentration, kBq/cm <sup>3</sup>	
		Surface <sup>*</sup>	bulk
I	0.21	$\geq 4.4\text{E}4$	2E2
II	1.9	7E5	5E3
III	10.1	4.9E6	2E4
IV	3.2	$\geq 4.0\text{E}5$	6E2
V	1.8	6.5E4	1.8E3

\* The concentration was measured for a layer of  $0.5\mu\text{m}$  to  $5\mu\text{m}$  thickness. For a layer of thickness larger than  $5\mu\text{m}$ , an uncertainty in the tritium concentration is indicated by a mark  $\geq$ .

For all the samples loaded with tritium at various temperatures the concentration in the surface layer was of approximately two order of magnitude larger than that in the bulk. The tritium depth profiles given in Fig.2 show tested samples having an enriched with tritium sub-surface layer of approx.  $15\div 20\mu\text{m}$  thickness. Amount of tritium counted in acid etching's cocktails resulted from removal of those layers presents 20% to 40% of the overall tritium inventory in the samples.

The observed tritium distribution is quite different from what could be expected in accordance with a classical mechanism of hydrogen diffusion in metals. For example, tritium profile calculated using the classical equation [3]

$$1 - C/C_S = \text{erf}(X/2[D \cdot t]^{0.5}) \quad (1)$$

(where  $C_S$  and  $C$  are tritium concentrations on the surface and at distance  $X$  from the surface,  $D$  is diffusion coefficient [12],  $t$  is time) for sample of series III shows that ratio  $C/C_S$  for a point of half sample's thickness should be  $\approx 0.9$ .

Tritium profiles presented in Fig. 7 to Fig. 11 for decontaminated samples also demonstrate presence of tritium-enriched sub-surface layer.

To explain the observed phenomena, it can be suggested that an unexpectedly large tritium concentration in a sub-surface layer might be caused by a non-classical mechanism of tritium penetration into the stainless steel. This penetration occurs even at room temperature, which means that tritium involved in such a process is more mobile than atomic hydrogen diffusing into a crystalline lattice of the stainless steel. A possible mechanism of the tritium penetration into a sub-surface layer could be an intergranular migration and trapping in defects of crystalline lattice, which concentrate at the surface of stainless steel. If this assumption is correct, an influence of micro-structural properties of stainless steel in sub-surface layer on tritium distribution might be expected.

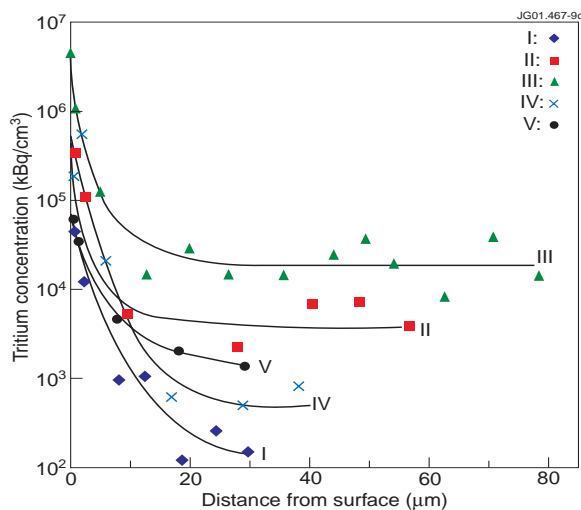


**Fig. 2** Tritium depth profile for samples of different series.

The thermal desorption spectrums show that a majority of tritium is released in a form of water vapor. This is in agreement with other thermal desorption studies [1,6,7,9,10]. As an example, the spectrum of the sample of series II is presented in Fig. 3. There were only one peak of HTO and two peaks of HT. The ratio of tritium released as HTO to that of HT was found 40, 150, 260 for samples of series I, II and III, which were loaded with tritium at temperature of  $\approx 295\text{K}$ ,  $470\text{K}$  and  $590\text{K}$  respectively. An increase of the ratio HTO/HT with rise of temperature of tritium loading could be attributed to increasing rate of reaction of oxygen in the “oxide” layer of the steel with hydrogen penetrated into the metal. The HTO/HT ratio for sample of series V, which was loaded with tritium under the same conditions as sample of the series III but was then baked-out at temperature of  $770\text{K}$  for 10 hours, was measured 15. A decrease of the HTO/HT

ratio for the baked-out sample could be caused by a chemical reaction between metal and tritiated water leading to metal oxidation and conversion of water to hydrogen. Another reason could be thermal desorption of tritium from the sample predominantly in a water form during the sample's baking-out followed by absorption of released tritium in reactor's wall [6,9]. The decreased tritium inventory for sample of the series IV, V (see Table 2) indicates that tritium desorption from the sample occurs during its baking-out. The temperature of baking-out was sufficient [1] for considerable tritium thermal desorption from the samples.

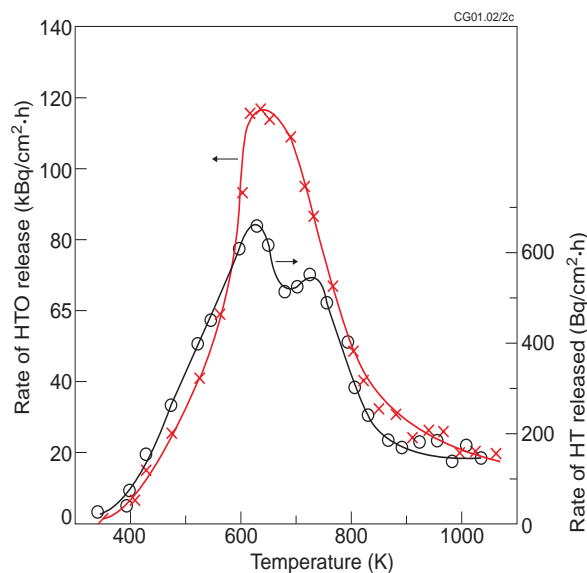


**Fig. 3** Thermal desorption spectrum of tritium released from sample of series II.

### 3.2 Tritium removal from stainless steel

Some results of study of tritium removal from stainless steel by gas-purge have been already presented elsewhere [13]. The kinetic curves of tritium recovery by the gas-purge at temperature of 570K presented in Fig. 4 show that rate of tritium removal increases in the row of the purge-gases:  $\text{Ar} < \text{Ar}/\text{H}_2 < \text{Air} < \text{Ar}/\text{NH}_3$ . The results of other decontamination tests are given in Table 3. It is well known [1] that water vapor is responsible for tritium removal from steel by purging with air. This means that oxidation of metal in reaction with oxygen does not contribute much to the detritiation process. Therefore tritium removal from the stainless steel can be attributed to two basic mechanisms, i.e. thermal desorption and isotopic exchange of tritium on the metal surface with hydrogen-containing gaseous species, such as hydrogen, water vapor, ammoniac used in this work. Separate study [14], in which the same rate of tritium removal from the stainless steel was observed for purging with argon containing water vapor at different partial pressures of 0.073Pa and 2.6kPa, showed that pressure of water vapor in purge-gas is not the factor predominantly determining rate of tritium removal. The increase of tritium removal rate for purge at temperature of 570K in row hydrogen, water vapor and ammoniac can be attributed to increase of activity of those reagents in isotopic exchange with tritium on the metal surface.

**Table 3** Results\* of the decontamination tests.

Sample and decontamination procedure	$A_R$	F
I-a: Ar/NH <sub>3</sub> -purge at 670K for 5.5 hours	150	0.75
I-b: Air-purge at 670K for 5.5 hours	170	0.85
I-c: Heating by flame for 10 seconds	200	≈1
II-a: Air-purge at 570K for 5.5 hours	1.7E3	0.89
II-b: Ar/NH <sub>3</sub> -purge at 570K for 5.5 hours	1.8E3	0.95
II-c: Ar/H <sub>2</sub> -purge at 570K for 5.5 hours	1.5E3	0.79
II-d: Ar-purge at 570K for 5.5 hours	1.3E3	0.68
II-e: Heating by flame for 10 seconds	1.9E3	≈1
III-a: Air-purge at 770K for 5.5 hours	6.4E3	0.63
III-b: Air-purge at 670K for 5.5 hours	8.6E3	0.85
III-c: Air-purge at 570K for 5.5 hours	9.1E3	0.9
III-e: Ar/H <sub>2</sub> -purge at 670K for 5.5 hours	6.4E3	0.64
III-f: Heating by flame for 10 seconds	9.3E3	0.92
IV-a: Heating by flame for 10 seconds	3.2E3	≈1
V-a: Air-purge at 570K for 5.5 hours	1.2E3	0.67
V-b: Heating by flame for 10 seconds	1.4E3	0.78

\*  $A_R$  is activity (kBq) removed from the sample, F is a fraction of tritium inventory removed from the sample.

Taking into account small difference between the rates of tritium removal by purging with Ar/NH<sub>3</sub> and air, simplicity of operation and processing of secondary waste, purging with an air containing a small amount of water vapor was considered as more attractive than purging with argon containing ammoniac. Tritium on the surface of stainless steel heated under air atmosphere participates in various reactions of isotopic exchange and recombination leading to removal of the tritium from the surface. Tritium of the sub-surface layer, which is enriched by tritium, migrates then to the decontaminated surface. This tritium can also migrate from the sub-surface layer deeper to the bulk. This means that an optimum temperature should exist for tritium removal due to competition between mentioned processes. Fig. 5 shows that this temperature is around 570K.

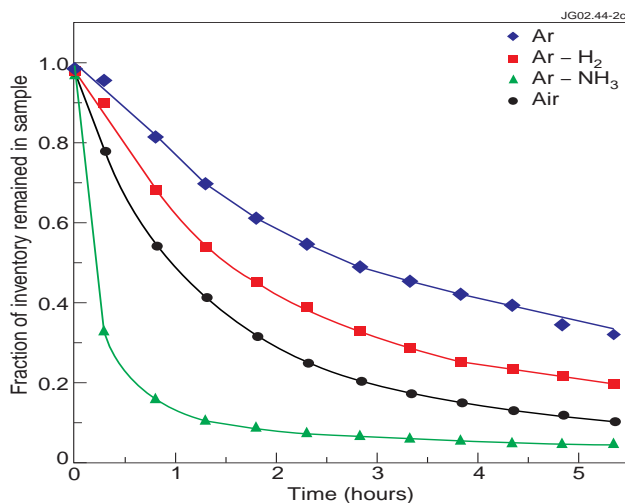


**Fig. 4** Kinetic curves of tritium recovery from samples of series II by purge with various gases at a temperature of 570K.

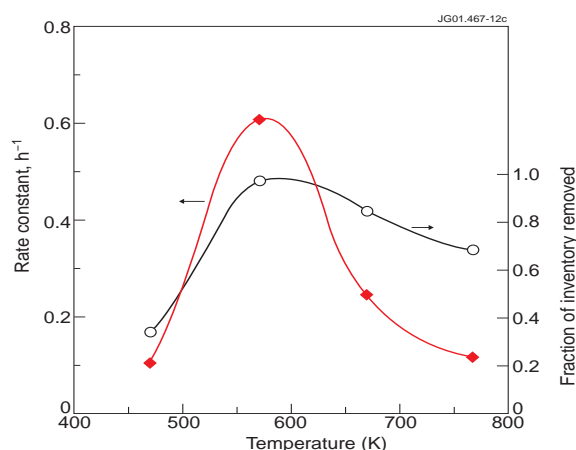


**Fig. 5** Rate constant of tritium removal and fraction of tritium removed by air-purge.

Tritium removal exhibits different behavior for samples of different thickness and conditions of tritium loading. Fig. 6 shows the kinetic curves of tritium recovery from the samples of series III and V. Fast detritiation of the sample of series III at the beginning of the air-purge can be attributed to tritium removal from the sub-surface layer enriched by a mobile tritium. Tritium removal from the sample of series V, in which larger fraction of hydrogen was transferred from water to hydrogen and driven more far from the surface, occurs slower than for sample of the series III and is most likely controlled by diffusion of atomic hydrogen from the bulk to the surface.

Review of Table 3 clearly shows that heating by flame allows removal of the largest fraction of tritium inventory and in a very short period of time. Increase of stainless steel thickness and baking-out of stainless steel pre-loaded with tritium make tritium removal more difficult. Acid etching of decontaminated samples revealed trace of internal oxidation for samples exposed to air at elevated temperatures.

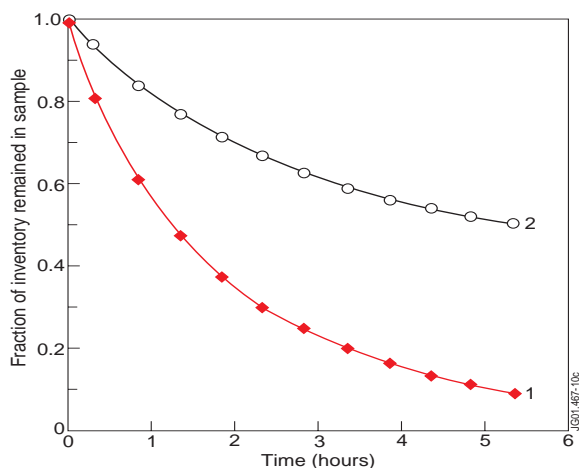


**Fig. 6** Kinetic curves of tritium removal from samples of series III (1) and V (2) by air-purge at a temperature of 570K.

Tritium depth profiles in the original and decontaminated samples are shown in Fig. 7-11. The profiles of decontaminated samples demonstrate presence of tritium-enriched sub-surface layer as it was observed for the non-decontaminated samples. For samples of series I and II,



where tritium in sub-surface layer contributes largely to the overall tritium inventory, tritium depth profiles are quite similar for samples decontaminated by different methods. For samples of series III, IV and V, where tritium is driven deeper to the bulk by loading at elevated temperature or baking-out of loaded samples, tritium depth profiles are different for samples decontaminated by different methods.

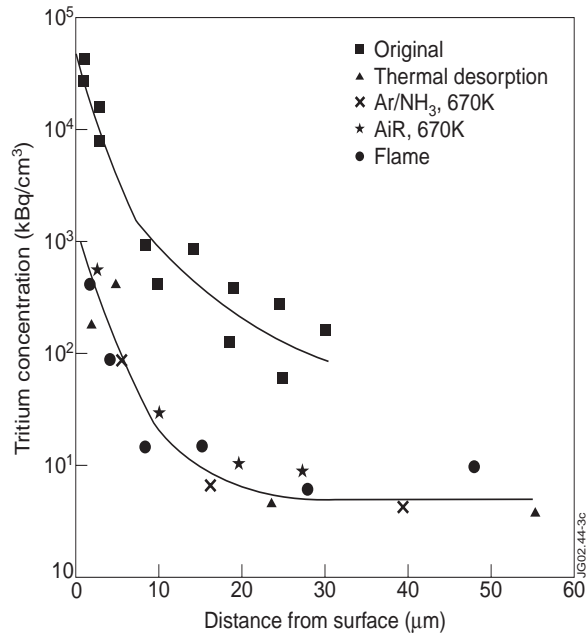


**Fig. 7** Tritium depth profile of the original and decontaminated samples of series I.

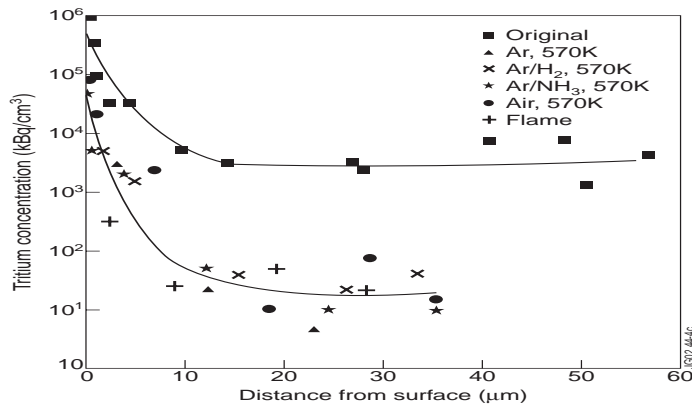


**Fig. 8** Tritium depth profile of the original and decontaminated samples of series II.

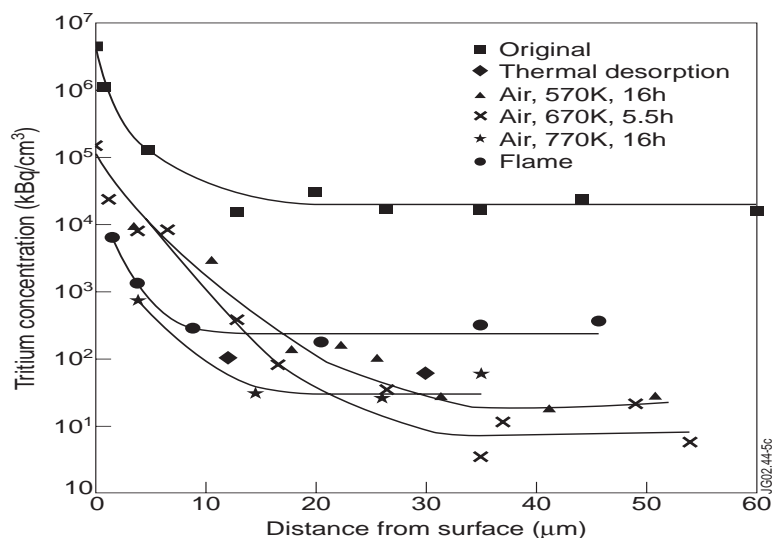


**Fig. 9** Tritium depth profile of the original and decontaminated samples of series III.

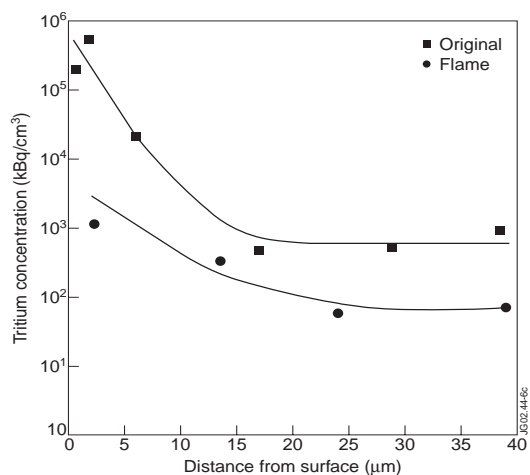


**Fig. 10** Tritium depth profile of the original and decontaminated samples of series IV.

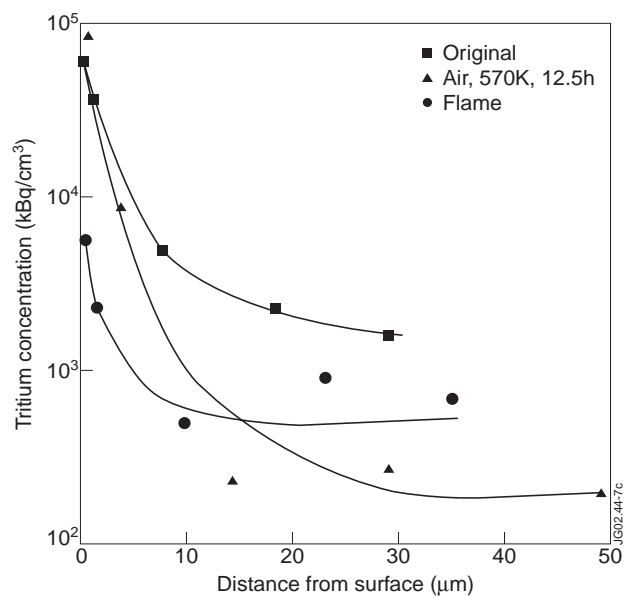


**Fig. 11** Tritium depth profile of the original and decontaminated samples of series V.

#### 4. Conclusions

1. Tritium distribution between surface and the bulk was studied for samples of stainless steel type 316 loaded by exposure to gaseous tritium-containing hydrogen at room and elevated temperatures. Tritium concentration of approximately two orders of magnitude exceeding the concentration in the bulk was found in the sub-surface layer of  $15 \div 20\mu\text{m}$  thickness. The tritium of the sub-surface layer contributes 20 to 40% to the overall tritium inventory. Easy tritium penetration into the sub-surface layer might be attributed to hydrogen intergranular migration and trapping in defects of crystalline lattice.

2. Detritiation by various methods, e.g. purging with air, argon, argon containing hydrogen or ammoniac, heating by methane-air flame, was tested. Heating by flame allows much quicker detritiation than gas-purging and larger fraction of tritium inventory removed. Two main mechanisms, i.e. thermal desorption and isotopic exchange with gaseous hydrogen-containing species, were considered determining the rate of tritium removal from the stainless steel by gas-purge. Activity increases in the row of hydrogen-containing agents, ie hydrogen, water vapor, ammoniac, being responsible for isotopic exchange with tritium on the metal surface. Taking into account additional efforts needed for processing of “secondary” waste, air was considered as a preferable agent for detritiation by gas-purge. There is an optimum temperature of  $\approx 570\text{K}$ , for tritium recovery from stainless steel by air-purge.

#### References

- [1] K.Y. Wong, B. Hircq, R.A. Jalbert and W.T. Shmayda, Fusion Engineering and Design **16** (1991) 159.
- [2] AC Bell, J. Williams, J. D. Neilson and A. Perevevnev, Fusion Science and Technology, **41** (2002) 626.
- [3] T. Hirabayashi and M. Saeki, J. Nucl. Mater. **120** (184) 309.
- [4] F. Ono, M. Yamawaki and S. Tanaka, Fusion Technology, **28** (1995) 1250.
- [5] R.A. Surette and R.G.C. McElroy, Fusion Technology, **14** (1988) 1141.
- [6] N.M. Masaki, T. Hirabayashi and M.Saeki, Fusion Technology **15** (1989) 1337.
- [7] T. Hirabayashi, M. Saeki and E. Tachikawa, J. Nucl. Mater. **126** (1984) 38.
- [8] T. Hirabayashi, M. Saeki and E. Tachikawa, J. Nucl. Mater., **127** (1985) 187.
- [9] A.B. Antoniazzi, W. T. Shmayda and R. A. Surette, Fusion Technology, **21** (1992) 867.
- [10] R.S. Dickson and J.M. Miller, Fusion Technology, **21** (1992) 850.
- [11] T. Hirabayashi, M. Saeki and E. Tachikawa, J. Nucl. Mater. **136** (1985) 179.

[12] F. Reiter, K.S. Forcey and G. Gervasini, Cat. No. CD-NA-15217-EN-C, ECSC-EEC-EAEC Brussels, (1993).

[13] A. Perevezentsev, K. Watanabe, M. Matsuyama and Y. Torikai, Fusion Science and Technology, **41** (2002) 706.

[14] Y. Torikai, A. Perevezentsev, M. Matsuyama and K. Watanabe, Fusion Science and Technology, **41** (2002) 736.